esa

ECOSPHERE

Surveying pasture communities in diachronic analyses by 3D models: the diachronic canopy variation model

Nicodemo G. Passalacqua,[1,†] Maurizio Muzzupappa,[2] Antonio Lagudi,[2] Liliana Bernardo,[1,3] Aldo Schettino,[4] and Domenico Gargano[1,3]

[1]*Museo di Storia Naturale della Calabria ed Orto Botanico, University of Calabria, Rende, Cosenza, Italy*
[2]*Department of Mechanical, Energetics and Management Engineering, University of Calabria, Rende, Cosenza, Italy*
[3]*Department of Biology, Ecology and Earth Science, University of Calabria, Rende, Cosenza, Italy*
[4]*Pollino National Park, Rotonda, Potenza, Italy*

Citation: Passalacqua, N. G., M. Muzzupappa, A. Lagudi, L. Bernardo, A. Schettino, and D. Gargano. 2019. Surveying pasture communities in diachronic analyses by 3D models: the diachronic canopy variation model. Ecosphere 10(3): e02613. 10.1002/ecs2.2613

Abstract. Aboveground biomass (AGB) is a parameter commonly used for assessing and monitoring primary productivity of grassland communities. Destructive AGB measurements, although accurate, are time-consuming and do not allow for repeated measurements as required by monitoring protocols. Structure-from-motion (SfM) photogrammetry has been proved to be a reliable tool for rapid and not destructive AGB estimations in grass systems. Three-dimensional (3D) models of fourteen 1×1 m^2 pasture plots were reconstructed and AGB volume measured under several measurement settings. Volume-based AGB measures were regressed to AGB values resulting from destructive methods to identify the measurement settings that show the best fit. Furthermore, 3D models of four mountain pasture plots were reconstructed in May, July, and August. Models relative to the same plot were aligned and their relative difference measured to produce a diachronic canopy variation model (DCVM). On the measured volume (V_d), the coefficient of density (c_ρ) was applied to adjust the volume values (V_{adj}) in relation to variation due to different DCVM point densities. The measurement setting for AGB volume estimations strongly influenced their correlation with traditional AGB scores. The best fit was obtained selecting 1 mm grid cell size and minimum point height distance. Such options were then selected to measure the DCVM. Adjusted volumes were fully correlated with the average point distance. Three plots revealed higher rates of AGB in the spring compared to summer season, as justified by the summer aridity constraints affecting vegetation productivity in Mediterranean areas. In one plot, we found an anomalous seasonal pattern, showing an AGB reduction in spring, which can be correlated with grazing, that promoted a subsequent increment in summer. Our study indicates that image-based photogrammetric techniques allow for reliable non-destructive measurements of surface biomass in diachronic analyses, offering a valuable tool for evaluating occurrence, magnitude, and spatial patterns of variations of community primary productivity over time. Diachronic canopy variation model produced congruent patterns of inter-seasonal canopy variations proving to be a useful tool for analyzing local disturbance to vegetation canopy caused by grazing.

Key words: biomass; coefficient of density; diachronic variation; local disturbance; non-destructive measurements; pasture community; photogrammetry; structure-from-motion.

Received 30 November 2018; accepted 14 January 2019. Corresponding Editor: Robert Washington-Allen.

† **E-mail:** nicodemo.passalacqua@unical.it

Introduction

Biodiversity and functioning of ecosystems are closely related to primary productivity: Biodiversity variations can result in a reduction of productivity (Tilman et al. 1996) and increases of biomass production can affect species diversity (Li et al. 2015). Therefore, monitoring primary productivity is crucial to understand how environmental variations affect ecosystems. Aboveground biomass (AGB), the most visible of the five carbon pools in terrestrial ecosystems (Ravindranath and Ostwald 2008), is widely used in ecological studies as a proxy of primary productivity. To this end, evaluating the AGB dry weight per unit surface is probably the most effective way to describe the primary productivity of an ecosystem. In highly responsive systems like grasslands, AGB estimations can help in (1) understanding the impact of biophysical and ecological processes on ecosystem productivity (Loreau and Hector 2001, Tilman et al. 2006) and (2) quantifying the effect of an array of biotic and abiotic factors on temporal and spatial productivity changes (Frank and McNaughton 1990, Augustine 2003, Knapp and Smith 2001). For such reasons, AGB estimation in grasslands is an effective tool for a wide range of ecological applications, including habitat monitoring (McNaughton 1985), pasture (Trotter et al. 2010) and fire management (Trollope et al. 1996), and carbon storage (Tilman et al. 2006).

From a methodological perspective, the most accurate way for estimating AGB requires cutting, drying, and weighting grass samples (Ohsowski et al. 2016). Despite the overall reliability, this usual procedure shows some relevant shortcomings. Indeed, it is time- and energy-consuming (Loudermilk et al. 2009), and it is destructive, by precluding chances for multitemporal replications of the measurements. Over time, ecologists tried to develop alternative methods for AGB estimations (Catchpole and Wheeler 1992). Disk pasture meter (Santillan et al. 1979) and point intercept method have often been used in vegetation studies as a reliable linear proxy of plant biomass (Frank and McNaughton 1990, Jonasson 1988, Chiarucci et al. 1999, Bråthen and Hagberg 2004).

More recently, techniques for three-dimensional (3D) reconstruction are receiving a growing interest, because they permit to obtaining a biomass estimation without using allometric information (Calders et al. 2015). Most studies deal with the use of the terrestrial laser scanning (TLS) technique to obtain a 3D point cloud of woody vegetation. Nonetheless, image-based 3D reconstruction (structure-from-motion, SfM; Snavely et al. 2008), widely applied in geosciences research and cultural heritage documentation, restoration, and conservation (Brutto and Meli 2012, Pollefeys et al. 2003, Bruno et al. 2017), appears an effective low-cost methodology alternative to laser-based systems (Westoby et al. 2012). Accordingly, the use of SfM is growing also in vegetation science, including landscape-scale analyses of dryland vegetation (Cunliffe et al. 2016) and tree structure evaluation (Morgenroth and Gomez 2014) while, to date, limited research exists in using image-based 3D reconstruction in the measurement of biomass in wild pastures.

Some authors (Hütt et al. 2014, Tilly et al. 2014) used 3D point clouds of herbaceous communities to assess grass height and to perform volume-based estimations of AGB, by finding out a meaningful correlation between measurements on models and destructively harvested data. Recent comparisons of AGB estimations for pasture communities resulted from SfM and TLS techniques (Wallace et al. 2017, Cooper et al. 2017) showed that both methods allow performing an accurate estimation of the surface biomass. However, to our knowledge no studies have used SfM to assess the diachronic AGB variations in highly diverse wild pasture communities, like those promoted by inter-seasonal climate variations in oro-Mediterranean habitats.

In highly diversified terrestrial systems as the Mediterranean mountain pastures, the application of SfM photogrammetry can undergo various technical limitations. Indeed, the high species diversity (>30 species/m^2) typical of these systems can form intricate vegetation structures where occlusions and shadows can result in an incomplete representation of their morphology. Moreover, adverse field conditions, such as the frequent presence of wind and the strongly variable light conditions, make difficult the acquisition of reliable data. Nonetheless, the availability of a low-cost fine surveying methodology would

strongly improve the knowledge and management of these valuable plant communities.

The aim of this work is to assess the effectiveness of the SfM photogrammetry to produce reliable fine-scale estimates of vegetation productivity (i.e., volume-based AGB variations) over time. The scope is to limit the methodological drawbacks originated by the vegetation removal implied by traditional AGB measures, which can constrain some analyses like multi-temporal monitoring. Specifically, diachronic canopy variation models (DCVMs) were defined to monitor the inter-seasonal productivity variations in plots representative of the Mediterranean mountain pasture in southern Italy.

Materials and Methods

Study area

Fieldwork was carried out in three sites over a period of 120 d from April to August 2015. The first site (Molinelle, MO: 39°21′25″ N, 16°13′45″ E, elevation 240 m. a.s.l.) was a thermophile Mediterranean community characterized by herbaceous species like *Dactylis hispanica*, *Bromus hordeaceus*, *Briza media*, *Medicago arabica* and *Trifolium* sp. pl. with vegetation cover ranging from 60% to 100% and average canopy height from 30 to 60 cm. The second site (Piano Ruggio, Mt. Pollino, PR: 39°54′41″ N, 16°7′45″ E) was a rich mesophilous mountain pasture dominated by *Festuca micriphilla* and *Dactylis glomerata*, and with high vegetation cover (from 70% to 100%). The third site (Mt. Serra, MS: 39°50′52″ N, 16°05′35″ E, elevation 1350 m s.l.m.) consisted in a mountain rocky pasture hosting a high plant diversity (Gargano et al. 2017). Here, the most frequent species included an array of grasses (e.g., *Festuca circummediterranea*, *Bromopsis erecta*, *Koeleria splendens*) and forbs (e.g., *Crepis lacera*, *Eryngium campestre*, *Armeria canescens*).

Plots of 1×1 m^2 were selected within each of the three study sites. Ten plots at MO, 2 at PR, and 2 at MS were collected in April 2015 for volume-to-biomass comparison (H), whereas further 4 plots (2 open to grazing, E, and 2 excluded from grazing by a fence, F) were collected in May, July, and August at MS for diachronic analysis.

The study communities show a vegetation cover ranging from 60% to 80%, with a canopy height of 50–70 cm. All the plots were on an almost flat surface (slope <5°) and marked at the corners with 30 cm tall vertical poles. The head of each pole was covered with a white strip to be clearly visible in the acquired images.

Image collection, pre-processing, and model reconstruction

The camera used to take images was a GoPro Hero 4 Silver model (GoPro, San Mateo, California, USA), an off-the-shelf, high-definition sports camera with a 12MP HD CMOS sensor. It was installed on top of a 1-m pole equipped with a Feiyu FY-G5 gimbal device (FeiyuTech, Guilin, China), to reduce pitch and roll movements and stabilize the acquisition. The camera was set in video mode, at a resolution of 1080 p at 60 frames per second (fps) and field of view of 108°. Two to four minutes of video recording was spent per each plot.

The camera network planned to survey the plots consists in open loop strips taken at about 10–15 cm above the maximum vegetation height. The camera was in downward-looking position and was moved horizontally right–left and left–right on overlapping strips along straight lines, ensuring a sidelap >30%. The occluded areas, not visible in downward-looking filming video, were acquired using oblique poses. To preserve the plots from wind and intense light contrast, they were sheltered with the flysheet of a free-standing tent before the acquisition (Quechua, 2 s 3 XL fresh & black).

A calibration procedure was performed to estimate the interior orientation parameters of the camera to reduce the distortion produced by the wide-angle lenses present on the GoPro Hero 4 and to improve the reconstruction process for the scene structure and the camera poses from images. For this purpose, we have used the commercial software Agisoft Lens (Agisoft; http://www.agisoft.com), an automatic lens calibration tool that supports the estimation of the full camera calibration matrix, including non-linear distortion coefficients.

All videos were fragmented into still frames, using VirtualDub software (VirtualDub v. 1.10.4; http://www.virtualdub.org). The fragmentation was performed using an extraction ratio of 1/30 fps, obtaining an average overlapping rate >60% between consecutive images.

Before the 3D reconstruction process, the data set has been processed through a three-step method. First, we used image enhancement techniques to increase the quality of the photogrammetric pipeline; in particular, a color balance and an exposure equalization algorithm were performed to have radiometrically calibrated images. Subsequently, the images were corrected for lens distortion using the undistortImage method implemented in the fisheye camera model of OpenCV (http://code.opencv.org/projects/opencv/wiki/VisionChallenge). The input vector of distortion coefficients had been determined in the previous calibration procedure.

Finally, the images were rectified using the Deshaker filter of VirtualDub software (VirtualDub v. 1.10.4) to solve the rolling shutter problem caused by the CMOS sensor present on the GoPro camera.

Structure-from-motion reconstructions were performed using the commercial software Agisoft PhotoScan Pro. In particular, the following photogrammetric pipeline was used to generate 3D point clouds:

1. The data set of images previously processed with the method described above was imported into PhotoScan. Then, an algorithm similar to Scale Invariant Feature Transform (Lowe 1999) was used to orient the images (i.e., retrieve the camera poses) and to build a sparse 3D reconstruction.
2. A local metric coordinate system based on Ground Control Points (GCPs) was set in PhotoScan to refine and reference the sparse 3D reconstruction. The head of the four poles placed at the corners of each plot was used as GCPs whereas their Euclidian coordinates were retrieved through a simple trilateration algorithm based on in situ measurements. In particular, a tape measure was used to determine the distance from the head of the poles to the ground surface, and between each pair of poles.

A non-linear optimization strategy, in which both camera pose and interior orientation parameters were adjusted, was applied to minimize error at GCP coordinates. The average root-mean-square error (RMSE) achieved at this step was 0.01 m for ground coordinates and 0.5 pixels for image coordinates. The GCP RMSE encompasses both errors in the GCP measures and intrinsic accuracy of the sparse SfM reconstruction.

3. Finally, a Multi-View Stereo (MVS) algorithm was used by PhotoScan to produce a dense 3D point cloud from the refined intrinsic orientation and ground-referenced camera exterior orientation.

Although the plots were on an almost flat surface (slope <5°), a normalization of the point clouds has been performed in order to derive the vegetation height. In particular, a planar representation of the ground surface was defined using the Euclidian coordinates of the four vertical poles as reference. Specifically, the measured distances from the head of each pole to the ground surface were subtracted from each z-coordinate in order to define the position of the ground surface at the base of each pole relative to the point clouds. To simulate the destructively harvested AGB estimation (see *Biomass weight* subsection of the *Materials and Methods* section), further 5 cm was subtracted from z-coordinates when vegetation volume was measured. A normalized vegetation height (NVH) was then determined based on the height of the point clouds above the identified ground surface.

Biomass weight

Fourteen 1×1 m^2 plots were used to test the relationship between fresh and dry biomass and volume measurements under different computational settings. After image collection, AGB at about 5 cm from the soil was cut and dried at 90°C in oven for 48 h. Removed biomass was weighted after cutting (fresh weight, FW) and after desiccation (dry weight, DW).

Canopy height and volume estimation

The volumetric surface differencing approach (Wallace et al. 2017), also called raster space (Cooper et al. 2017), was used for volume measurements. This method does not require full canopy penetration but assumes that the space beneath the points to the ground surface is occupied by vegetation. It involves the creation of a digital model representing the top of the surface biomass. Raster grids were generated by partitioning the x, y plane of the point cloud into square cells. The volume is then calculated as the

product of the cell area and the cell height which is derived from the NVH value of the points falling within that cell.

The volume estimation was expected to be sensitive to the cell dimensions. In this work, a cell grid size of 1, 5, 10, 20, and 50 mm and minimum and maximum NVH values (MinH and MaxH, respectively) were selected to find the best setting to be used for volume estimation.

Diachronic canopy variation model

The seasonal productivity and the structural variations over time of the four mountain pasture plots selected for the diachronic analysis (see subsection 2.1) were estimated by measuring the canopy height and the volume differences occurring in each plot during a specific time frame. This was achieved through a direct comparison of the 3D point clouds referred to the same plot by defining a new 3D model, the DCVM.

To create the DCVM, 3D point clouds representing the same plot, but in different dates, were processed using CloudCompare software (CloudCompare 2.7.0, http://www.cloudcompare.org). First, they were aligned by using a target-based registration approach. This technique is based on the detection of homologous geometrical entities (features) among the 3D reconstructions of the same plot and their subsequent alignment. For this purpose, we used the vertical poles placed at the corner of each plot.

This operation (Registration, Tools menu) was repeated several times until the 3D point clouds were fully overlapping on *x*-, *y*-, and *z*-axes. Homologous points clearly observable on 3D models (e.g., rocks laying on the ground) were selected (Point picking, Tools menu) and their Euclidean coordinates compared in order to assess the alignment accuracy; an RMSE below 2 mm was considered as acceptable.

Once alignment was set, point clouds were cleaned to remove all points outside the perimeter of the field plot (Segment, Edit menu). Moreover, a visual checking to identify changes in the stone arrangement and/or soil removal/accumulation due to animal activities (cows, bears, etc.) was performed; we did not find any significant change on the ground surface to be removed before the volume measurement.

Finally, the DCVM was created by applying the volumetric surface differencing approach (Volume, Tools menu) using as reference the first 3D point cloud of the time series. In particular, once cell grid size and cell height parameters were set, based on the best fitting results achieved from the volume-to-biomass relationship (see subsection 3.3), the model was defined and exported as a 3D point cloud.

Data analysis

The initial quality of the point clouds was determined through a visual inspection, by assessing the point density and their position in 3D space to determine how well the vegetation structure was represented.

Subsequently, statistical parameters were extracted from the harvested plots and used to evaluate different settings for volume calculation. Specifically, volume measurements were regressed to FW and DW biomass using the coefficient of determination (r^2), the probability test (P), and the relative RMSE (rRMSE) in order to determine which setting had the best performance and assess how different settings in volume calculation influence the relationship between biomass and volume.

The relative heights of the 3D points belonging to the DCVMs were exported and statistically analyzed using Data Desk 6.3.1 software (Data Description, Ithaca, New York, USA). A volume variation (V_d) of a plot during a specific time frame was then estimated as the sum of the relative heights extracted by the relative DCVM. However, considering that the volume calculation is closely related to the number of corresponding points, we adjusted the estimation by using a coefficient of density (c_ρ) defined as

$$c_\rho = \rho_{max}/\rho$$

where ρ_{max} is the value of the maximum DCVM density, while ρ is the density of the relative DCVM. This approach assumes that missing grid cells have the same height distribution as the generated cells in the considered DCVM. As a consequence, the adjusted volume (V_{adj}) can be defined as

$$V_{adj} = c_\rho V_d.$$

Finally, V_d and V_{adj} values were regressed on the average values of the DCVM cell heights to verify the improvement of the volume variation estimate due to the introduction of the coefficient

of density c_ρ. To observe the spatial distribution of the canopy height variation, a chromatic scale was associated with the cell height value.

Results

Data collection and processing

The equipment used for data collection has proved to be useful during fieldwork activities. GoPro camera is small (100 × 40 × 60 mm) and light (350 g), and it is easily kept in the rucksack, with an additional battery too. The tent is light (2.5 kg), but a bit bulky (cover: 89 cm diameter × 9 cm thickness), resulting slightly uncomfortable to carry across shrub vegetation. Setting up the tent on the plot was very quick (<5 min), but the presence of intense wind created several difficulties, increasing the required time up to 15–20 min. The use of the tent had proved to be crucial since plots were efficiently protected from wind and changeable solar lighting, which are two constants in the mountain environment.

The field data capture, including equipment setting and video recording, took 5–7 min per plot. Specifically, a total time of 1–1.5 h was requested to collect the four plots used for the diachronic analysis, from our arrival to our leaving.

Video recording produced 10,000–18,000 frames per plot. We selected about 750 frames per plot obtaining an overlapping rate >60% between consecutive frames; this took about 30 minutes per plot. The manual selection of the images was necessary to extract consistently good still frames from video and avoid blurry and out-of-focus shots. Three-dimensional point cloud generation required a processing of about 24 h per plot.

Point cloud properties

Point cloud density was very high, ranging from about 500,000 to 3,000,000 points/m^2 (Table 1), providing a good representation of the vegetation structure. Indeed, it was possible to recognize most structural details of the community, including several isolated elements over the top of the canopy (flowering stems, seed heads, small leaves; Fig. 1; Video S1). Moreover, using the textured 3D mesh representation of the plots, it was possible to recognize most dominant and large species, but also many small ones. Of course, individuals laying under the community canopy were not observable.

Volume-to-biomass analysis

Biomass harvested in the 14 plots ranged between 288 and 2383 g for FW and between 53 and 428 g for DW, with a DW/FW biomass ranging between 0.14 and 0.66 (Table 1). Regression of DW on FW biomass was high (r^2 = 84.0%, rRMSE = 11.5%). Different cell grid size settings showed two diverse trends related to the height point setting (Table 2, Fig. 2). Using MaxH, volume measurements tend to increase linearly with cell grid size (Table 2, Fig. 2a), rising the data dispersion (see σ in Table 2). Minimum height distance setting exhibited non-linear correlation (Table 2, Fig. 2b), with a clear upward break moving from 1 mm to 5 mm cell size and a linear decrease from 5 to 50 mm cell size, albeit the dispersion of data was similar in this latter four settings (σ ranging from 114 to 133). Regressing volumes to biomass, MinH was always significantly related to biomass and showed a better fitness with respect to MaxH (Table 2). The best performance was at 1 mm cell grid size and MinH, for both DW (Fig. 3a) and FW (Fig. 3b; r^2 = 70.4 and 66.3%; rRMSE = 17.8% and 19.1%, respectively). Increments in cell grid size corresponded to a general decrease in biomass correlations, becoming not significant when volumes were measured with larger cell grid size under MaxH. As a consequence, 1 mm cell grid size and MinH were selected for DCVM.

Table 1. Values in harvested plots (H) of dry (DW) and fresh (FW) aboveground biomass, their ratio (DW/FW), and point cloud density after refining.

Plot	FW (g)	DW (g)	DW/FW	Density (points/m^2)
H1	2383	428	0.180	905,037
H2	1356	227	0.167	429,770
H3	1506	268	0.178	969,908
H4	1005	141	0.140	1,011,277
H5	1158	173	0.149	902,685
H6	476	75	0.158	725,778
H7	293	53	0.181	1,170,516
H8	288	58	0.201	799,008
H9	602	127	0.211	731,657
H10	551	109	0.198	498,114
H11	112	74	0.661	999,961
H12	320	171.7	0.537	3,148,876
H13	552	180.5	0.327	1,457,701
H14	556	164.8	0.296	1,037,852

Fig. 1. Structure-from-motion aligned 3D point clouds clipped to a 1 × 1 m area from (a) oblique, (b) nadir, and (c) profile view. Data shown for plot H1.

Diachronic canopy variation model

In the four field plots, variations from the end of May to the beginning of July, representing variations occurring in the spring period, and from the beginning of July to mid-August, representing variations of summer period, were analyzed. Eight DCVMs were generated, with point density ranging from about 200,000 to 540,000 points/m^2, excluding F2 summer that was 85,379 points/m^2 (Table 3). In all DCVMs, point height distributions failed the normality test (Kolmogorov-Smirnov test: $P = 0$) and showed a similar standard deviation (σ ranging from 0.020 to 0.047; Table 3). Volumes were well correlated with the average values of the DCVM cell heights (Fig. 4a), and they raised to a full linear correlation adjusting the volume by the coefficient of density (Fig. 4b).

In the spring period, fenced plots had a significant increase in average canopy height and a positively tailed distribution (Table 3, Fig. 5a, b). Average height was 2.1 and 3.1 cm and volume difference 11.6 and 6.3 dm^3, respectively. The contrasting pattern observed in F2, higher average height and lower volume with respect to F1, disappeared once the F2 volume was standardized by the coefficient of density (Table 3; Vol_{adj}). Plots open to grazing showed a different pattern: E2 had a little increase in average canopy height and volume, whereas E1 had a decrease with an evident secondary peak in the left side of the histogram (Table 3, Fig. 5c).

Summer period showed an average increment in canopy height in plot E1 and, in a minor way, in plot F1 (Table 3). In both plots, point height distribution was positively tailed (Fig. 6a, c), but plot E1 showed a secondary peak on the right side of the histogram. This secondary peak included height increases ranging from 6 to 15 cm, occurring manly in the same area where the spring decrement was detected (compare Fig. 5c and 6c). Average canopy height and volume increment (V_{adj}) were almost the same of the decrement values observed in the spring season. E2 showed a very low decrement in canopy height and volume, with 50% of cell heights ranging between −1.16 and 0.8 cm (Table 3, Fig. 6d), whereas F2 had the higher decrement in both average height and volume. In F2, a widespread decrease occurred in the plot (50% of heights below −2.56 cm and 25% between −2.6 and 0.36 cm; Table 3, Fig. 6b, blue areas). In contrast, in F1 a relevant decrement interested 25% of the cells, while 50% of cells showed no or little increase, and the remaining 25% of cells increased substantially (Table 3, Fig. 6a, red areas).

Table 2. AGB volume statistics and correlation with fresh (FW) and dry (DW) weight biomass of 14 harvested plots at different grid cell size (mm) and point height distance settings.

Distance	Grid size (mm)	Volume (dm^3)		FW		DW	
		μ	σ	r^2	rRMSE (%)	r^2	rRMSE (%)
MaxH	1	38.1	11.6	62.9***	23.6	59.7**	25.1
	5	72.4	27.9	46.3**	62.7	32.5*	69.3
	10	85.2	34.8	36.3*	83.0	23.7	90.0
	20	103.8	44.5	27.6	>100	17.0	>100
	50	146.2	65.3	21.9	>100	13.3	>100
MinH	1	34.1	9.2	66.3***	17.8	70.4***	19.1
	5	41.7	13.3	53.3**	26.0	50.9**	27.1
	10	36.8	13.3	46.8**	29.2	47.0**	28.5
	20	29.3	12.7	42.6*	30.2	47.0**	29.9
	50	17.9	11.4	40.7*	28.3	51.2**	28.8

Notes: MaxH: maximum distance; MinH: minimum distance; μ: mean; σ: standard deviation; r^2: coefficient of determination; rRMSE: relative root-mean-square error.
$^{***}P < 0.001$; $^{**}P < 0.01$; $^{*}P < 0.5$.

Discussion

The primary advantages of using the outlined image-based method for the AGB estimation are the low cost of the equipment and a reduction in field and processing time in comparison with the other techniques. Nonetheless, wind disturbance during image acquisition process represents one of the major limitations in the application of SfMs to pasture communities, because point cloud reconstructions require widely overlapping images of non-moving objects (Cooper et al. 2017). From a practical point of view, the equipment and procedure used in the present work were successful in overtaking this restriction. Fencing the plot with a tent, and using a user-friendly action camera, despite being fixed to a pole, resulted in high-quality models of the pasture plots. Average point cloud density was over 1,000,000 points/m^2 in harvested plots and about 350,000 points/m^2 in DCVMs. Such values are quite comparable, or better, to those obtained using high-resolution digital cameras. For instance, the models of Cooper et al. (2017) produced an average cloud density of about 40,000 points per 0.5 × 0.5 m plot, corresponding to 160,000 points/m^2, while models by Wallace et al. (2017) reached about 195,000 points in circular plots with a radius of 0.15 m, corresponding to 690,000 points/m^2. These outcomes are really encouraging for applying such fine-scale modeling techniques in adverse environmental contexts, which are often of great interest for biodiversity monitoring. Using a tent involves a limitation in the applicability of the approach, which is restricted to herbaceous plant communities. Plot size and plant community height that can be fenced depend on the tent size. A large tent could allow image acquisition of wider areas and taller plants, but it would require a careful evaluation of the limitations derived by the weight to carry up in the field and the time needed to setting up the tent.

Although the harvested plots were highly variable in structure and AGB (DW ranging from 74 to 428 g), the volume-based AGB estimates obtained from our 3D models were highly correlated with real biomass measurements (r^2 = 70.4%, rRMSE = 19.07). Such correlation score was comparable to that resulted in Wallace et al. (2017; r^2 = 72%, rRMSE = 21.7%), and in Cooper et al. (2017; r^2 = 72%, on total AGB, 54% on grass AGB, rRMSE not available), who worked with considerably smaller plots. Working with excessively small plots can overlook fine-scale productivity variations related to local resource heterogeneity. This could be a substantial limitation in species-rich wild communities. Indeed, soil resource heterogeneity is a major driver of crucial community processes (i.e., patterns of species assembly and primary productivity) and an effective modulator of ecosystem responses against environmental variations (García-Palacios et al. 2012). Therefore, working

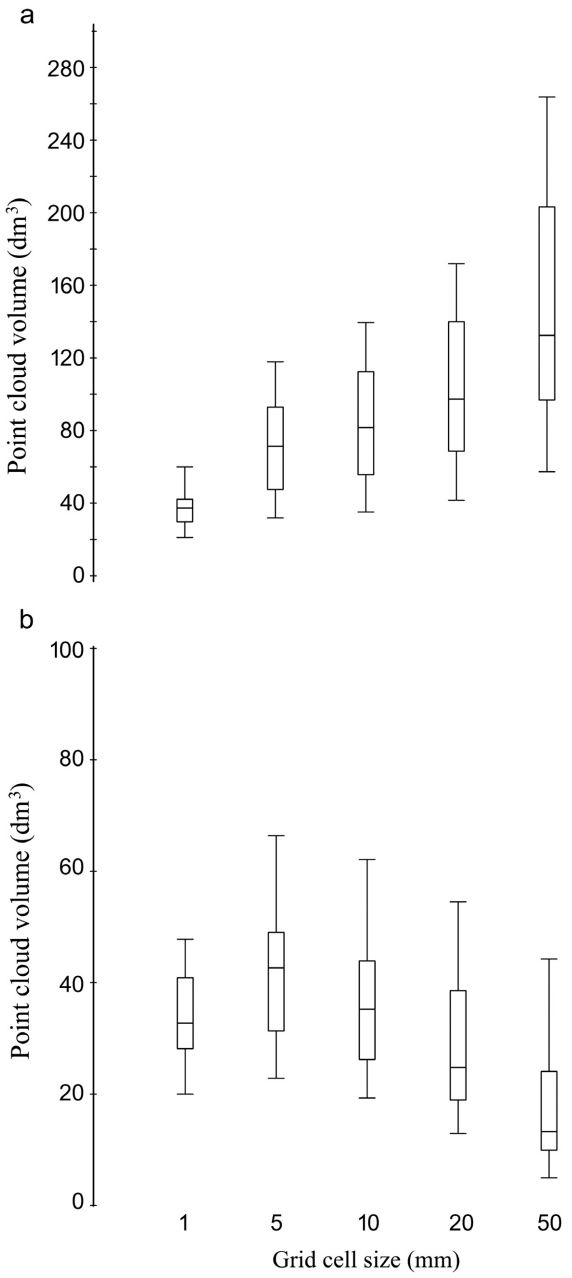

Fig. 2. Box plots of AGB volumes (dm^3) measured at different grid cell size (mm) in harvested plots. (a) MaxH and (b) MinH.

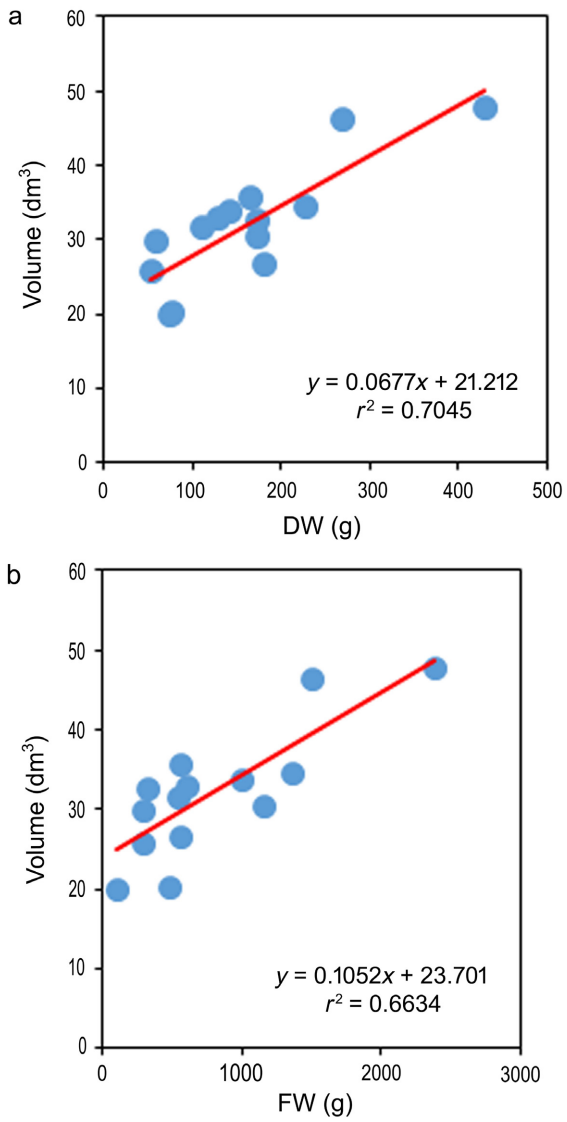

Fig. 3. Regression relationship between AGB volume and dry weight biomass (DW): volume measured at 1 mm grid cell size and (a) minimum (MinH) and (b) maximum (MaxH) point height distance.

with quite large plots can help in capturing a sufficient amount of such variability in AGB estimations carried out from SfM applications.

The predictive power of AGB estimations strongly depended on the volume computation setting (i.e., cell size, point height distance). The best correlation was obtained by using the minimum point height distance at 1 mm cell size. Increments in cell grid size, and the use of the maximum point height distance, resulted in reduced r^2 and increased rRMSE (Table 2). This finding partially agrees with Wallace et al. (2017), who found the best correlation in pasture communities at the smallest tested cell size

Table 3. Diachronic canopy variation model (DCVM) statistics, from May to June (spring), and from June to August (summer): average point height distance (μ) and standard deviation (σ), measured (V_d) and adjusted (V_{adj}) volumes, and their ratio with the average, in fenced (F) and open (E) to grazing plots.

DCVM	Density	μ (cm)	σ	V_d (dm^3)	Vol/μ	V_{adj} (dm^3)	Vol_{adj}/μ
F1 spring	540,192	2.14	3.47	11.6	5.4019	11.6	5.4019
F2 spring	206,296	3.05	4.34	6.3	2.0630	16.5	5.4019
E1 spring	482,618	−1.88	3.69	−9.1	4.8262	−10.1	5.4019
E2 spring	536,430	0.70	2.34	3.8	5.3643	3.8	5.4019
F1 summer	290,150	1.18	4.04	3.4	2.9015	6.4	5.4019
F2 summer	85,379	−2.61	4.74	−2.2	0.8538	−14.1	5.4019
E1 summer	296,088	2.05	3.56	6.1	2.9609	11.1	5.4019
E2 summer	356,580	−0.15	2.01	−0.5	3.5658	−0.8	5.4019

(5 mm) on maximum height, but is in contrast to Cooper et al. (2017), where the best correlation occurred at intermediate tested cell size (20 mm) on average point height. However, differences in plot shape and size, as well as in the methods used to set community parameters like AGB dry weight and volume, complicated the comparison of data obtained from different works. Hence, due to the effect on final estimates, further work is needed to define the most suitable setting when computing point cloud volume.

If SfMs provide an innovative technique for estimating aboveground primary productivity, its use for diachronic analyses on community productivity is an absolute novelty. Spatiotemporal dynamics of AGB are a key topic in research on global change impact on terrestrial ecosystems (Steffen et al. 1998). In effect, AGB rates represent a reliable indicator of vegetation status, for which temporal variations reflect ecosystem responses to changes in environmental drivers like climate (Roy et al. 2001). Due to intra-annual climate dynamics, pasture communities undergo substantial seasonal biodiversity variations (Vymazalová et al. 2012, Gargano et al. 2017) which are likely to affect their responsiveness to ongoing environmental changes (Gargano et al. 2017). Nonetheless, little is said about the related dynamics of aboveground primary productivity. Traditional AGB approaches could fail in monitoring such dynamics due to the limitations caused by biomass harvesting. Non-disturbing techniques based on AGB proxies derived from remote-sensed data are a consistent way to analyze temporal dynamics of primary productivity (Jiao et al. 2017), but their efficacy could be limited for fine community-scale applications. Therefore, SfMs can supply a powerful way to investigate local AGB temporal patterns. It is important to note that DCVM density was lower than in harvested plots. This gap depended on the computational method required to generate the DCVMs. Indeed, if a column of the grid has no point in the earlier cloud or in the later cloud, that column is not generated in the DCVM, resulting in a reduction of point density. However, we overcame such a shortcoming by applying the coefficient of density, which assumes that height distribution of missing cells follows the same distribution of generated cells. The correspondence between the adjusted volume and the average point height highlighted the importance of considering point density in DCVMs, by supporting the adjusted volume as the better proxy of AGB weight. In this way, our diachronic models produced congruent patterns of inter-seasonal canopy variations by overtaking the limitations due to vegetation harvesting for evaluating aboveground plant biomass. Plots E2, F1, and F2 revealed higher rates of AGB in the spring compared to summer season, as justified by the summer aridity constraints affecting vegetation productivity in Mediterranean areas (Mitrakos 1980).

In addition, DCVMs appeared a useful tool for analyzing local disturbance to vegetation canopy caused by grazing. Overall, the AGB estimates from DCVMs highlighted that spring vegetation growth was more pronounced in fenced plots compared to open ones, a possible effect of the biomass harvested by herbivores in the previous years. In addition, the models suggested that grazing can modify the normal seasonal dynamics of vegetation productivity. Indeed, the anomalous

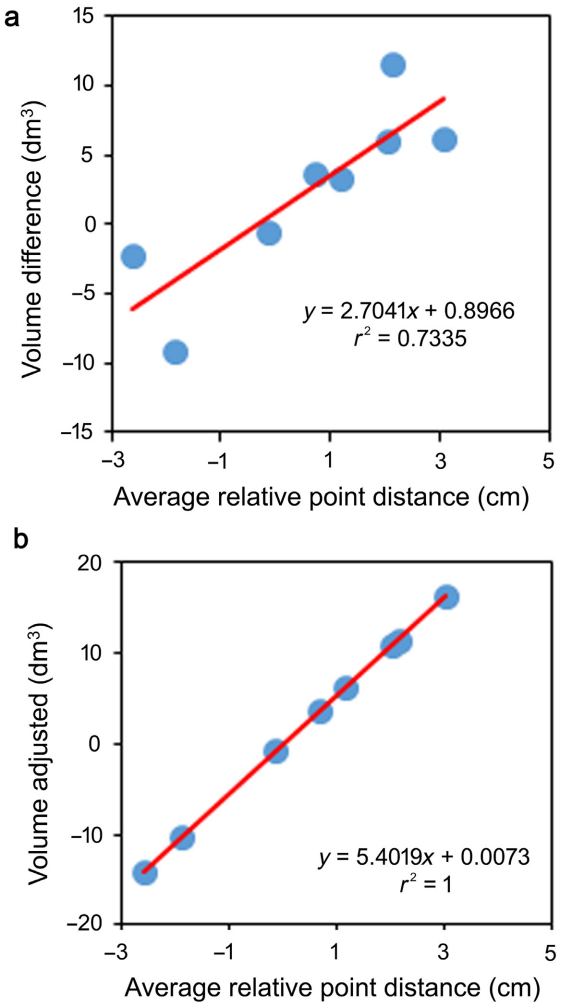

Fig. 4. Regression relationship between (a) volume differences (V_d), and (b) adjusted volume differences (V_{adj}), and average relative point height distance in diachronic canopy variation models.

seasonal patterns found in the plot E1 (i.e., AGB reduction of AGB in the spring and increment of AGB in the summer) were related to spring grazing. Accordingly, in the areas of the plot showing a spring reduction of canopy height (Fig. 5c), we detected a subsequent increment of vegetation volume in the summer (Fig. 6c). Moreover, the corresponding histogram indicated that this grazing event promoted a late peak of vegetation growth (Fig. 6c). Grazing pressure linked to traditional pastoral systems is a crucial ecological driver for pasture and grassland communities, as both excess and absence of grazing can result in a loss of biodiversity and quality of these herbaceous communities (Dullinger et al. 2003, Mayer et al. 2009). Current patterns of grazing intensity are contradictory, as elevated grazing intensities can locally occur also in regions where grazing is generally reducing (Gargano et al. 2012). Because aboveground primary productivity is a fundamental indicator for determining the sustainable use of grassland resources (White et al. 2000, O'Mara 2012), our findings open further perspectives in the use of SfMs for fine-scale surveying of grazing pressure.

Conclusion

Estimation of pasture community AGB is important for understanding and managing landscapes which are continually altered by anthropogenic and natural processes. Structure-from-motion photogrammetry has been proved to be a reliable tool for not destructive AGB estimations in grass systems. The results of the present research are encouraging in order to explore new possible applications of SfM photogrammetry in the ecological field, such as the use for AGB estimation in mountain pasture communities and in diachronic analyses.

The application of SfM to mountain pasture communities poses some technical problems, such as the frequent presence of wind, the variable and strongly contrasted brightness, and the site not accessible by car, and requires the use of suitable tools. We used a tent, to fence the plot from wind and solar irradiation, and an action camera, to acquire images all over the plot with the operator sitting in a fixed point. The combination of a tent and an action camera allowed the acquisition of enough defined images that were aligned by the software. The resulted point clouds showed a high point density (500,000–3,000,000 points/m^2).

A volumetric surface differencing approach was used to derive grass volumes from the 3D point clouds. We tested several computational settings, such as different grid cell size and point height distance. Volume-based AGB measures were regressed to AGB values obtained by destructive methods to identify the measurement setting with the best fit. We obtained the higher correlation selecting 1 mm grid cell size and the minimum point height distance (r^2 = 70.4% and

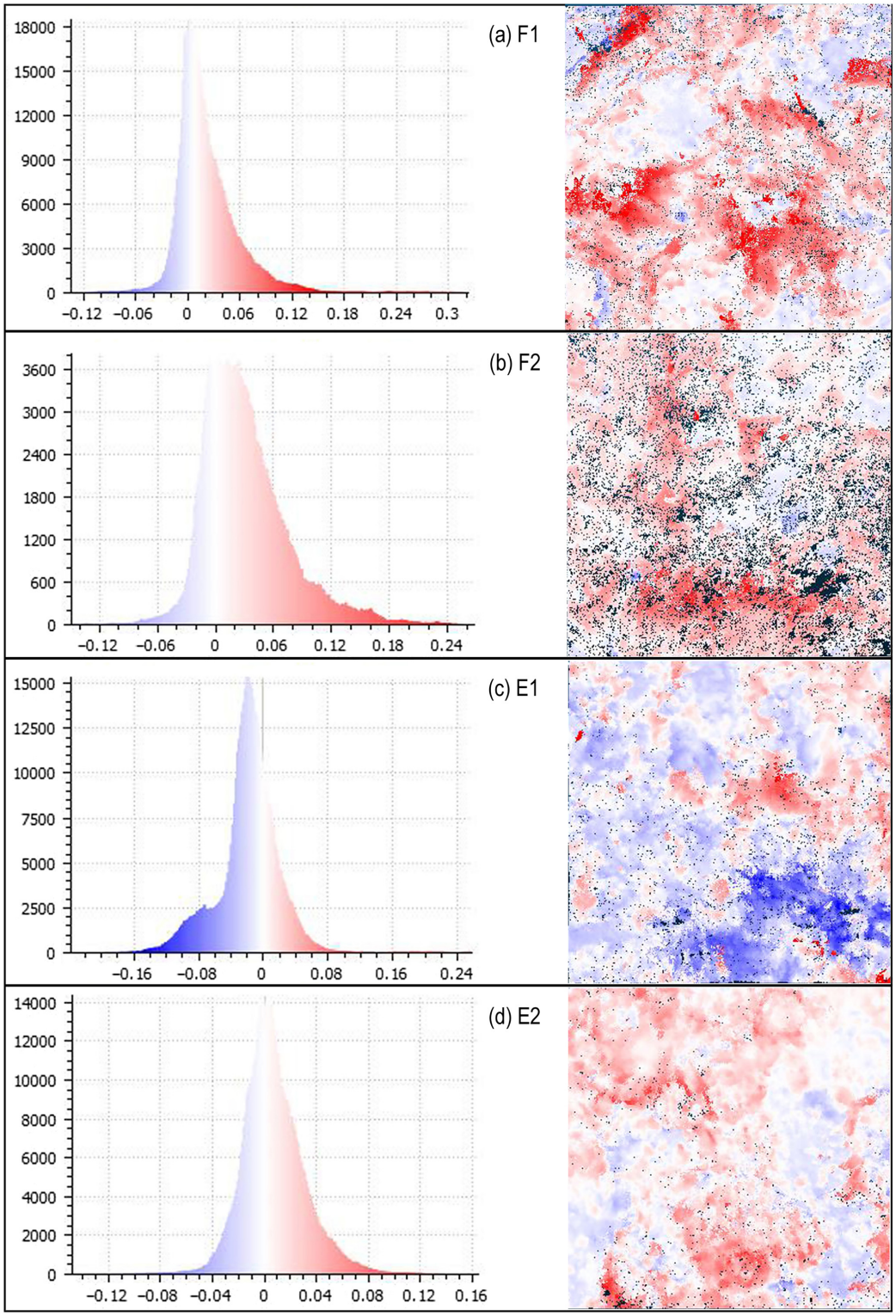

Fig. 5. Histogram (left) and top view (right) of relative point height distance of diachronic canopy variation models in the spring period: F1 (a), F2 (b), E1 (c), and E2 (d).

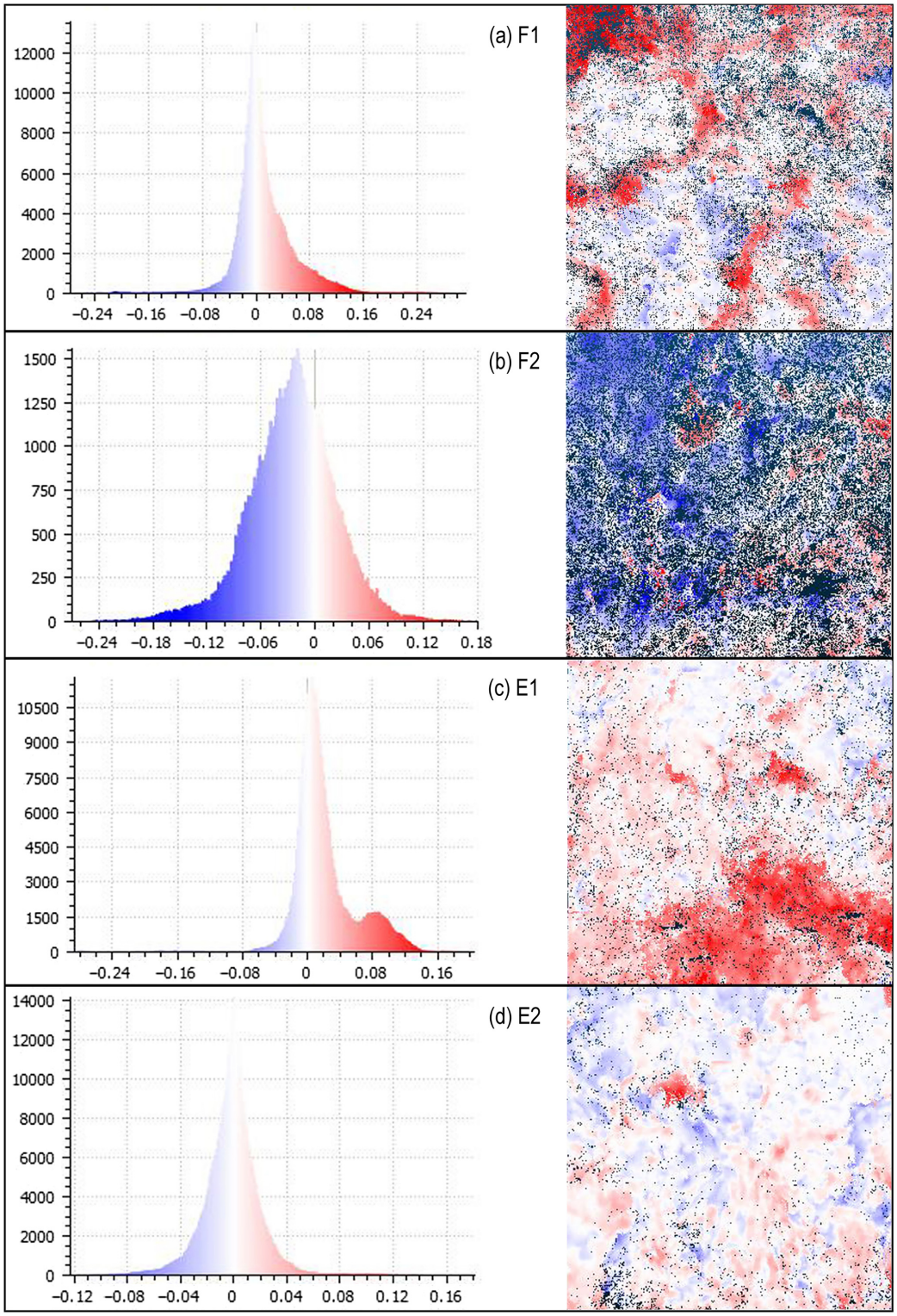

Fig. 6. Histogram (left) and top view (right) of relative point height distance of diachronic canopy variation models in the summer period: F1 (a), F2 (b), E1 (c), and E2 (d).

rRMSE = 19.1%). Reducing the grid cell size resulted in significant but lower correlations, whereas selecting maximum point height distance the correlation, at each grid cell size, was lower with respect to the minimum point height distance, and not significant when combined with larger grid cell sizes. Such options were then selected for measures in diachronic analyses.

Destructive AGB measurements do not allow for repeated measurements as required by monitoring protocols. In this study, a method for analyzing diachronic variations in biomass was developed and tested in two environmental conditions (open and fenced plots) and in two time spans, spring season (May–July) and summer season (July–August). Models relative to the same plot were aligned in order to produce DCVMs, setting the earlier 3D model as ground field and measuring the relative differences. Diachronic canopy variation models resulted in having a high point density variability, due to a shortcoming in the computational method, that affected the measured volumes and making them not comparable. On the measured volume (V_d), we applied the coefficient of density (c_ρ), which is the ratio between the density of a defined plot and the higher density among all considered plots, obtaining a full correlation of the adjusted volume to the average point height. Diachronic models produced congruent patterns of inter-seasonal canopy variations by overtaking the limitations due to vegetation harvesting for evaluating aboveground plant biomass. Three plots revealed higher rates of AGB in the spring compared to summer season, as justified by the summer aridity constraints affecting vegetation productivity in Mediterranean areas. Aboveground biomass estimates highlighted that spring vegetation growth was more pronounced in fenced plots compared to open ones, a possible effect of the biomass harvested by herbivores in the previous years, and the fourth plot showed an AGB reduction in the spring, and an increment of AGB in the summer, likely related to spring grazing.

Our study indicates that image-based photogrammetric techniques allow for reliable nondestructive measurements of surface biomass in diachronic analyses, offering a valuable tool for evaluating occurrence, magnitude, and spatial patterns of variations of community primary productivity over time.

Further research to establish optimal methodologies for SfM data acquisition and for volume variation estimation in pasture communities is recommended.

Acknowledgments

We thank the Pollino National Park for the financial support and the operative assistance during the fieldwork.

Literature Cited

Augustine, D. J. 2003. Spatial heterogeneity in the herbaceous layer of a semi-arid savanna ecosystem. Plant Ecology 167:319–332.

Bråthen, K., and O. Hagberg. 2004. More efficient estimation of plant biomass. Journal of Vegetation Science 15:653–660.

Bruno, F., L. Barbieri, A. Lagudi, M. Cozza, A. Cozza, R. Peluso, and M. Muzzupappa. 2017. Virtual dives into the underwater archaeological treasures of South Italy. Virtual Reality 22:91–102.

Brutto, M. L., and P. Meli. 2012. Computer vision tools for 3D modelling in archaeology. International Journal Heritage in the Digital Era 1:1–6.

Calders, K., G. Newnham, A. Burt, S. Murphy, P. Raumonen, M. Herold, D. Culvenor, V. Avitabile, M. Disney, and J. Armston. 2015. Nondestructive estimates of above-ground biomass using terrestrial laser scanning. Methods in Ecology and Evolution 6:198–208.

Catchpole, W., and C. Wheeler. 1992. Estimating plant biomass: a review of techniques. Australian Journal of Ecology 17:121–131.

Chiarucci, A., J. B. W. Wilson, B. J. Anderson, and V. Dominicis. 1999. Cover versus biomass as an estimate of species abundance: Does it make a difference to the conclusions? Journal of Vegetation Science 10:35–42.

Cooper, S. D., D. P. Roy, C. B. Schaaf, and I. Paynter. 2017. Examination of the potential of terrestrial laser scanning and structure-from-motion photogrammetry for rapid nondestructive field measurement of grass biomass. Remote Sensing 9:531.

Cunliffe, A. M., R. E. Brazier, and K. Anderson. 2016. Ultra-fine grain landscape-scale quantification of dryland vegetation structure with drone-acquired structure-from-motion photogrammetry. Remote Sensing Environment 183:129–143.

Dullinger, S., T. Dirnböck, J. Greimler, and G. Grabherr. 2003. A resampling approach for evaluating effects of pasture abandonment on subalpine plant species diversity. Journal of Vegetation Science 14:243–252.

Frank, D., and S. McNaughton. 1990. Above-ground biomass estimation with the canopy intercept method—a plant-growth form caveat. Oikos 57:57–60.

García-Palacios, P., F. T. Maestre, R. D. Bardgett, and H. de Kroon. 2012. Plant responses to soil heterogeneity and global environmental change. Journal of Ecology 100:1303–1314.

Gargano, D., S. Aiello, T. Abeli, A. Schettino, and L. Bernardo. 2017. Monitoring biodiversity patterns in three Mediterranean mountain pastures in the Pollino National Park (S-Italy). Plant Sociology 54:51–59.

Gargano, D., A. Mingozzi, A. Massolo, S. Rinaldo, and L. Bernardo. 2012. Patterns of vegetation cover/dynamics in a protected Mediterranean mountain area: influence of the ecological context and protection policy. Plant Biosystems 146:9–18.

Hütt, C., H. Schiedung, N. Tilly, and G. Bareth. 2014. Fusion of high resolution remote sensing images and terrestrial laser scanning for improved biomass estimation of maize. The International Archives of the Photogrammetry, Remote Sensing and Spatial Information Sciences 40:101.

Jiao, C., G. Yu, J. Ge, X. Chen, C. Zhang, N. He, Z. Chen, and Z. Hu. 2017. Analysis of spatial and temporal patterns of aboveground net primary productivity in the Eurasian steppe region from 1982 to 2013. Ecology and Evolution 7:5149–5162.

Jonasson, S. 1988. Evaluation of the point intercept method for the estimation of plant biomass. Oikos 52:101–106.

Knapp, A. K., and M. D. Smith. 2001. Variation among biomes in temporal dynamics of aboveground primary production. Science 291:481–484.

Li, W., J. M. Cheng, K. L. Yu, H. E. Epstein, L. Guo, G. H. Jing, J. Zhao, and G. Z. Du. 2015. Plant functional diversity can be independent of species diversity: observations based on the impact of 4-yrs of nitrogen and phosphorus additions in an alpine meadow. PLoS ONE 10:e0136040.

Loreau, M., and A. Hector. 2001. Partitioning selection and complementarity in biodiversity experiments. Nature 412:72–76.

Loudermilk, E. L., J. K. Hiers, J. J. O'Brien, R. J. Mitchell, A. Singhania, J. C. Fernandez, W. P. Cropper, and K. C. Slatton. 2009. Ground-based lidar: a novel approach to quantify fine-scale fuelbed characteristics. International Journal of Wildland Fire 18:676–685.

Lowe, D. G. 1999. Object recognition from local scale-invariant features. Pages 1150–1157 *in* B. Werner, editor. Computer vision 1999. The proceedings of the seventh IEEE international conference on. Volume 2. IEEE, Los Alamitos, California, USA.

Mayer, R., R. Kaufmann, K. Vorhauser, and B. Erschbamer. 2009. Effects of grazing exclusion on species composition in high-altitude grasslands of the Central Alps. Basic and Applied Ecology 10:447–455.

McNaughton, S. 1985. Ecology of a grazing ecosystem: the Serengeti. Ecological Monographs 55:259–294.

Mitrakos, K. 1980. A theory for Mediterranean plant life. Acta Oecologica 1:245–252.

Morgenroth, J., and C. Gomez. 2014. Assessment of tree structure using a 3D image analysis technique —A proof of concept. Urban Forestry & Urban Greening 13:198–203.

Ohsowski, B. M., K. E. Dunfield, J. N. Klironomos, and M. M. Hart. 2016. Improving plant biomass estimation in the field using partial least squares regression and ridge regression. Botany-Botanique 94:501–508.

O'Mara, F. P. 2012. The role of grasslands in food security and climate change. Annals of Botany 110:1263–1270.

Pollefeys, M., L. Van Gool, M. Vergauwen, K. Cornelis, F. Verbiest, and J. Tops. 2003. 3D capture of archaeology and architecture with a hand-held camera. The International Archives of the Photogrammetry, Remote Sensing and Spatial Information Sciences 34:262–267.

Ravindranath, N. H., and M. Ostwald. 2008. Carbon inventory methods: handbook for greenhouse gas inventory, carbon mitigation, and roundwood production projects. Advances in global change research. Volume 29. Springer, Dordrecht, The Netherlands.

Roy, J., H. A. Mooney, and B. Saugier, editors. 2001. Terrestrial global productivity. Academic Press, Stanford, California, USA.

Santillan, R. A., W. Ocumpaugh, and G. Mott. 1979. Estimating forage yield with a disk meter. Agronomy Journal 71:71–74.

Snavely, N., S. M. Seitz, and R. Szeliski. 2008. Modeling the world from internet photo collections. International Journal of Computer Vision 80:189–210.

Steffen, W., et al. 1998. The terrestrial carbon cycle: implications for the Kyoto Protocol. Science 280:1393–1394.

Tilly, N., D. Hoffmeister, Q. Cao, S. Huang, V. Lenz-Wiedemann, Y. Miao, and G. Bareth. 2014. Multitemporal crop surface models: accurate plant height measurement and biomass estimation with terrestrial laser scanning in paddy rice. Journal of Applied Remote Sensing 8:083671.

Tilman, D., J. Hill, and C. Lehman. 2006. Carbon-negative biofuels from low-input high-diversity grassland biomass. Science 314:1598–1600.

Tilman, D., D. Wedin, and J. Knops. 1996. Productivity and sustainability influenced by biodiversity in grassland ecosystems. Nature 379:718.

Trollope, W. S. W., L. A. Trollope, A. F. L. Potgieter, and N. Zambatis. 1996. Safari-92 characterization of biomass and fire behavior in the small experimental burns in the Kruger National Park. Journal of Geophysical Research: Atmospheres 101:23531–23539.

Trotter, M. G., D. W. Lamb, G. E. Donald, and D. A. Schneider. 2010. Evaluating an active optical sensor for quantifying and mapping green herbage mass and growth in a perennial grass pasture. Crop and Pasture Science 61:389–398.

Vymazalová, M., I. Axmanová, and L. Tichý. 2012. Effect of intra-seasonal variability on vegetation data. Journal of Vegetation Science 23:978–984.

Wallace, L., S. Hillman, K. Reinke, and B. Hally. 2017. Non-destructive estimation of above-ground surface and near-surface biomass using 3D terrestrial remote sensing techniques. Methods in Ecology and Evolution 8:1607–1616.

Westoby, M. J., J. Brasington, N. F. Glasser, M. J. Hambrey, and J. M. Reynolds. 2012. 'Structure-from-Motion' photogrammetry: a low-cost, effective tool for geoscience applications. Geomorphology 179:300–314.

White, R., S. Murray, and M. Rohweder. 2000. Pilot analysis of global ecosystems: grassland ecosystems. World Resources Institute, Washington, D.C., USA.

Supporting Information

Additional Supporting Information may be found online at: http://onlinelibrary.wiley.com/doi/10.1002/ecs2.2613/full